EUROGRAPHICS Workshop on Graphics and Cultural Heritage (2019)
S. Rizvic and K. Rodriguez Echavarria (Editors)

Short Paper

Lens Calibration for Focus Shift Correction in Close-Range Multispectral Imaging

S. Brenner[1] and R. Sablatnig[1]

[1]TU Wien, Institute of Visual Computing & Human-Centered Technology

Abstract

Multispectral imaging has become a popular tool to reveal properties and structures in cultural heritage objects that are hidden to the human observer. One of the inherent problems of multispectral imaging applications is chromatic aberration. Due to an extended spectral range, the effect appears more pronounced than in conventional photography in the visible spectrum. This paper is concerned with longitudinal chromatic aberrations, i.e. shifts of the focal plane along the principal axis of the camera, as they are hard to correct in post-processing and should be avoided during acquisition. To this end, a calibration scheme to measure the wavelength- and distance-dependent focal shift behavior of a given camera/lens system is proposed, which allows for a mechanical compensation at acquisition time. The approach is demonstrated on a multispectral imaging system for historical manuscript analysis. We show that the application of this compensation approach enables the acquisition of in-focus images in non-visible wavelengths using a lens optimized for the visible spectrum only.

CCS Concepts

• ***Applied computing*** → *Arts and humanities;* • ***Hardware*** → *Sensors and actuators; Displays and imagers;*

1. Introduction

Multispectral imaging has become a widely used tool for the analysis of cultural heritage objects, such as manuscripts or paintings [TSAS*19]. It is used to recover faded writings or palimpsests [FSS*12, HDF*15, Kno18], or reveal covered layers of ink or paint [GCL*19]. An inherent problem of multispectral imaging is caused by optical dispersion: the refractive indices of materials depend on the wavelenght of the refracted light [ŠKB*10, MN13]. In imaging, this effect manifests as chromatic aberrations, leading to both offsets between color channels in the image plane (lateral chromatic aberration) and offsets of their focal planes (longitudinal chromatic aberration) [JF06]. In the extreme case of multispectral images, where the range of utilized wavelengths typically ranges from ultraviolet to infrared, the effect is pronounced. While it is possible to design lenses that minimize chromatic aberrations between certain wavelengths [HM63, MN13], it is impossible to completely eliminate aberrations for the whole optical spectrum utilized for multispectral imaging; furthermore, such specialized lenses are not always available or feasible for a given application.

Lateral aberrations, whether caused by dispersion, application of optical filters [BSA08] or other influences, can be corrected in post-processing via conventional image registration procedures or by using prior information from dedicated geometric calibration [ŠKB*10]. On the other hand, information is lost irreversibly when channels are out-of-focus. Extensive research has been done on deblurring images by deconvolution [CE07, PF16]. While Heide et al. [HRH*13] show that chromatic aberrations in images taken with simplistic lenses can be greatly reduced using such methods, frequencies that have been entirely eliminated by convolution (i.e. multiplied by zero in frequency space) cannot be restored by deconvolution. It is therefore desirable to avoid focus shifts at acquisition time. While the practical effect of focus shifts can be reduced by choosing a smaller aperture and thus increasing the depth of field, this approach faces its limits: first, diffraction-induced blur increases with decreasing aperture size; second, a small aperture can lead to unfeasible exposure times or the necessity of increased illumination intensities, which is problematic for sensitive objects such as manuscripts.

In this paper, we propose a novel approach to the problem, consisting in the measurement and modeling of the focal shift behavior of a given lens, allowing for its mechanical compensation. To this end, we introduce a lens calibration procedure that measures shifts of the focal plane for a set of wavelengths and working distances. These measurements are used to establish functions that allow the determination of focus shifts under a given wavelength for arbitrary working distances. This information is subsequently used to correct for dispersion-induced focus shifts at acquisition time.

The remainder of the paper is structured as follows: Section 2 introduces the calibration procedure and Section 3 demonstrates its practical application, with an evaluation given in Section 4. Section 5 discusses problems of the approach and proposes solutions, while Section 6 draws final conclusions.

DOI: 10.2312/gch.20191342

2. Calibration Procedure

Apart from the properties of the lens (which we view as a black box), the magnitude of focus shift Δ with respect to a reference wavelength λ_0 depends on both the employed wavelength λ and the distance d between camera and object. Thus, the proposed calibration procedure aims at producing a function $\Delta(\lambda, d)$ describing the behavior of a given lens without any knowledge of its inner structure. We find this function by fitting to a set of empirical measurements.

To measure the focus shift for a given configuration (λ, d), a calibration object is used. It consists of a target plane that is placed perpendicular to the principal axis of the camera, and a ruler plane, which is tilted by 45° with respect to the target plane (see Figure 1). Thus, when viewed from the camera, a known length l on the ruler corresponds to a difference in depth of $l/\sqrt{2}$. To measure a focus shift with respect to a reference wavelength λ_0, the camera is first focused on the reference plane under λ_0. Subsequently, an image is taken under another wavelength λ_i. The focus shift for λ_i in real-world units can be directly read by finding the sharpest area of the ruler in the corresponding image.

Figure 1: *Calibration object. For our experiments we used a commercially available product designed for autofocus calibration.*

In this way, a series of measurements is performed: For each wavelength $\lambda_i, 1 \leq i \leq M$ relevant to the respective imaging system and for several distances $d_j, 1 \leq j \leq N, N \geq 3$ within the typical working range, an image $I_{i,j}$ is taken and used to measure the focus shift $\hat{\Delta}_{i,j}$. This procedure is summarized in Algorithm 1.

Data: wavelengths λ_i, sample distances d_j,
Result: samples $\hat{\Delta}_{i,j}$ of the unknown function $\Delta(d, \lambda)$
for $j \in [1, N]$ **do**
  place target plane at distance d_j from the camera;
  focus on target plane under reference wavelength λ_0;
  for $i \in [1, M]$ **do**
    take image $I_{i,j}$ under wavelength λ_i;
    $\hat{\Delta}_{i,j} \leftarrow$ focus shift read from ruler in $I_{i,j}$;
  end
end

Algorithm 1: *Outline of the calibration procedure.*

In a typical multispectral imaging setting the utilized wavelengths are limited to a discrete set (defined by an available set of optical filters [Cos15] and/or narrow-band light sources [Kno18]), but the imaging distance can be varied continuously according to the individual use-case. It is therefore practical to consider individual one-dimensional functions $\Delta_i(d)$ per wavelengths λ_i, instead of the joint two-dimensional function $\Delta(\lambda, d)$. We found that $\Delta_i(d)$ are well approximated by quadratic polynomials of the form $\Delta_i(d|\boldsymbol{\theta_i}) = \boldsymbol{\theta_i}\,[d^2\ d\ 1]^T$. The parameter vector $\boldsymbol{\theta_i} \in \mathbb{R}^3$ is found via least-squares fitting to the measured data by minimizing:

$$\min_{\boldsymbol{\theta_i}} \sum_{j=1}^{N} (\hat{\Delta}_{i,j} - \Delta_i(d_j|\boldsymbol{\theta_i}))^2.$$

Under knowledge of the current object distance, the thus found functions are used to compute the magnitude of the relative focus shift Δ for a given imaging configuration. This focus shift describes the distance the focus plane moves in real-world space; it can thus be mechanically compensated by either adjusting the distance between camera and object or the focal distance of the lens by $-\Delta$.

3. Experimental results

The approach described in Section 2 was used to calibrate a multispectral image acquisition system tailored for the imaging of historical manuscripts, consisting of a *PhaseOne IQ260 Achromatic* camera system equipped with a *Schneider-Kreuznach 120mm ls f/4.0 Macro* lens, and multispectral LED panels producing 11 wavebands from 365nm to 940nm.

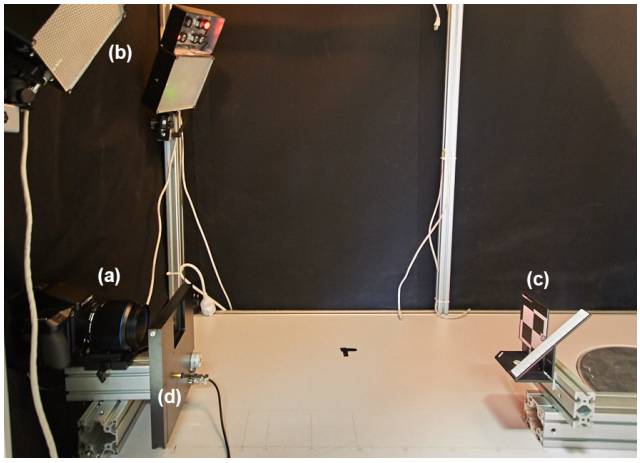

Figure 2: *Calibration setup consisting of the camera (a), multispectral light sources (b) and the calibration object (c). An optical filter wheel (d) is necessary to block fluorescent light when imaging in the ultraviolet range.*

For the reference focus on the target plane, a single wavelength from the center of the visible spectrum (535nm) was chosen as λ_0. Five wavelengths from the ultraviolet (365nm) and infrared (700nm, 780nm, 870nm and 940nm) ranges were known to produce noticeable focus shifts for our camera system and thus considered for calibration. Distance samples were taken in 100mm steps

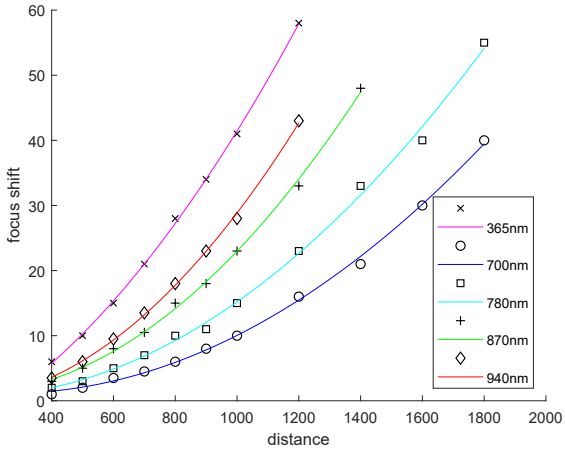

Figure 3: *Measurements and fitted functions (axis units in millimeters).*

λ (nm)	365	700	780	870	940
RMSE (mm)	0.4522	0.5616	1.0608	0.6531	0.4607
R^2	0.9995	0.9984	0.9970	0.9985	0.9991

Table 1: *Root mean squared errors (RMSE) and coefficients of determination (R^2) of the fitted functions.*

from 400 to 1000mm, and in 200mm steps from 1000 to 1800mm. To ease the identification of the sharpest areas on the ruler, a large aperture of f/4 was used. As a calibration object, the commercially available *Spyder LensCal* that is originally designed for autofocus calibration (see Figure 1), was used. Figure 2 shows the full setup during calibration.

In this experiment, the focus shift magnitudes were read from the images of the tilted ruler manually. Figure 3 shows the obtained measurements and the fitted quadratic polynomials. Note that above 1200mm working distance, some measurements are missing because the focus plane shifted beyond the depth region covered by the ruler plane. The root mean squared errors and coefficients of determination of the fitted functions with respect to the measurements are listed in Table 1.

To test the focus shift compensation, the lens was first focused on the target plane under λ_0. For any wavelength included in the calibration, the focus was adjusted according to the respective estimated function by driving the auto focus motor via the camera API. As Figure 4 shows, the implementation of the proposed calibration and subsequent compensation into our system allows the acquisition of in-focus images in the ultraviolet and infrared range, even though the camera lens used is not optimized for that purpose.

4. Evaluation

To test the feasibility of a quadratic polynomial for modeling the focus shift with respect to object distance, a series of exhaustive cross-validations was performed. Table 2 shows the results. Polynomials of degrees 1-5 were fitted to different subsets of the distance samples and tested on the remaining ones. The values shown in the table aggregate results of all wavelengths and possible selections of N samples from the total number of measurements. It can be observed that for more than three training samples, the 2^{nd} degree polynomial best describes the data, while the other tested models over- or underfit. Furthermore the table shows the expected errors when calibrating the system with a reduced number of distance samples.

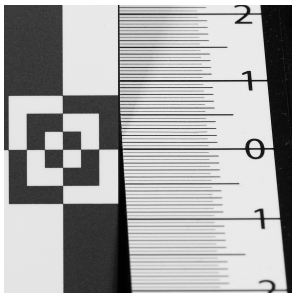

(a) *reference image at 535nm*

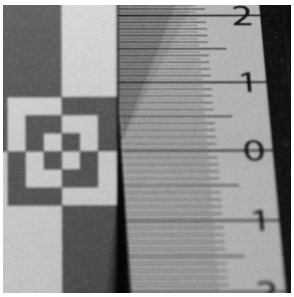

(b) *365nm, without correction*

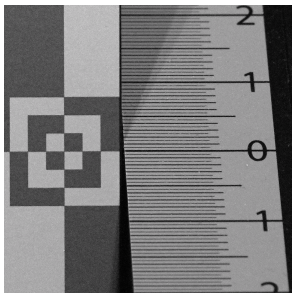

(c) *365nm, corrected*

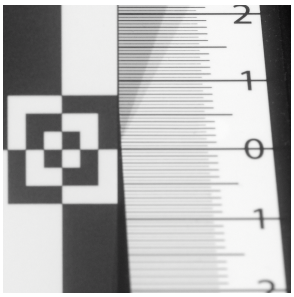

(d) *940nm, without correction*

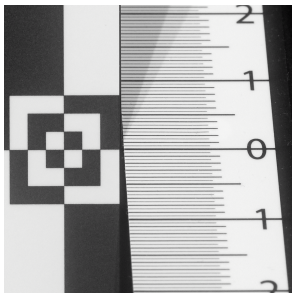

(e) *940nm, corrected*

Figure 4: *Images acquired with our multispectral imaging system: the reference image at 535nm (a), ultraviolet (b,c) and infrared (d,e) images without and with correction. Images taken from 1m distance with an aperture of f/8.*

5. Discussion

As shown in the previous sections, the proposed calibration and correction approach is suitable to enable the acquisition of sharp images outside the visible spectrum under usage of imperfect lenses. The model errors shown in Table 1 lie in the order of 1mm or

N	degree 1	degree 2	degree 3	degree 4	degree 5
2	11.37				
3	**9.01**	12.20			
4	8.26	**5.16**	85.84		
5	7.06	**4.66**	8.58	402.39	
6	6.79	**3.55**	31.68	157.12	1778.73
7	6.04	**1.83**	2.49	80.81	688.40
8	4.60	**0.74**	3.37	13.61	53.53
9	3.54	**1.02**	1.78	4.15	13.05
10	2.99	**0.70**	0.99	2.05	4.10

Table 2: *Results (RMSE) of exhaustive cross-validations for different choices of polynomials. N measurements were used for training, 11 − N for testing. The lowest error for each value of N is bold.*

below; this is well below the magnitude of depth variations that are to be expected in the surfaces of manuscripts or paintings, which makes the model accurate enough for the application at hand.

However, the presented implementation exhibits shortcomings, one of which is the amount of manual intervention required in the calibration procedure. During image acquisition, the distance between camera and calibration object must be adjusted for the sampling of different focal distances. This was done manually in our experiments, but the automation using a linear positioning unit is straight-forward. Furthermore the reading of focus shifts from the acquired images was done manually for our experiments, which is a time-consuming and error-prone task when performed by a human. However, we expect that the automation of this task with computer vision methods is solvable with limited engineering effort: it includes retrieving the pose of the calibration object with known texture and geometry, and detecting the area of maximum focus in the binarily textured ruler plane. Depending on the requirements of the application, the calibration process can be accelerated further by reducing the number of distance samples (see Table 2).

Another issue to consider is the change in image scale when adjusting the camera-object distance or the focal distance, as this introduces misalignments between spectral layers. However, as mentioned in Section 1, misalignments can also occur for other reasons, such as lateral chromatic aberrations or the application of optical filters. Hence, fine-registration is a sensible pre-processing step of any multispectral image processing pipeline, regardless if an explicit focus correction takes place or not.

6. Conclusion

In this paper a simple yet effective approach to compensate focus shifts induced by chromatic aberrations in close-range multispectral imaging setups is proposed. A multispectral imaging system corrected with the proposed method is capable of producing in-focus images when working with wavelengths the camera lens has not been optimized for. A calibration has to be carried out only once for a given camera system and remains valid for various spatial imaging configurations. While in our experiments the practical execution of the calibration procedure required some manual intervention, we have proposed approaches to eliminate them; their implementation and verification is considered future work.

References

[BSA08] BRAUERS J., SCHULTE N., AACH T.: Multispectral filter-wheel cameras: Geometric distortion model and compensation algorithms. *IEEE Transactions on Image Processing 17*, 12 (2008), 2368–2380. doi:10.1109/TIP.2008.2006605. 1

[CE07] CAMPISI P., EGIAZARIAN" K.: *Blind image deconvolution. Theory and applications*. 2007. doi:10.1201/9781420007299. 1

[Cos15] COSENTINO A.: Panoramic, Macro and Micro Multispectral Imaging: An Affordable System for Mapping Pigments on Artworks. *Journal of Conservation and Museum Studies 13*, 1 (2015), 1–17. doi:10.5334/jcms.1021224. 2

[FSS*12] FAIGENBAUM S., SOBER B., SHAUS A., MOINESTER M., PIASETZKY E., BEARMAN G., CORDONSKY M., FINKELSTEIN I.: Multispectral images of ostraca: Acquisition and analysis. *Journal of Archaeological Science 39*, 12 (2012), 3581–3590. doi:10.1016/j.jas.2012.06.013. 1

[GCL*19] GRIFONI E., CAMPANELLA B., LEGNAIOLI S., LORENZETTI G., MARRAS L., PAGNOTTA S., PALLESCHI V., POGGIALINI F., SALERNO E., TONAZZINI A.: A new infrared true-color approach for visible-infrared multispectral image analysis. *Journal on Computing and Cultural Heritage 12*, 2 (2019). doi:10.1145/3241065. 1

[HDF*15] HOLLAUS F., DIEM M., FIEL S., KLEBER F., SABLATNIG R.: Investigation of Ancient Manuscripts based on Multispectral Imaging. *DocEng 2015 - Proceedings of the 2015 ACM Symposium on Document Engineering*, 1 (2015), 93–96. doi:10.1145/2682571.2797072. 1

[HM63] HERZBERGER M., MCCLURE N. R.: The Design of Superachromatic Lenses. *Applied Optics 2*, 6 (1963), 553. doi:10.1364/ao.2.000553. 1

[HRH*13] HEIDE F., ROUF M., HULLIN M. B., LABITZKE B., HEIDRICH W., KOLB A.: High-quality computational imaging through simple lenses. *ACM Transactions on Graphics 32*, 5 (2013), 1–13. doi:10.1145/2516971.2516974. 1

[JF06] JOHNSON M. K., FARID H.: Exposing digital forgeries through chromatic aberration. *Proceedings of the Multimedia and Security Workshop 2006, MM and Sec'06 2006*, 2 (2006), 48–55. doi:10.1145/1161366.1161376. 1

[Kno18] KNOX K. T.: Image Processing Software for the Recovery of Erased or Damaged Text. *Manuscript Cultures 11* (2018), 63–72. 1, 2

[MN13] MIKS A., NOVÁK J.: Method for primary design of superachromats. *Applied Optics 52*, 28 (2013), 6868–6876. doi:10.1364/AO.52.006868. 1

[PF16] PERRONE D., FAVARO P.: A Clearer Picture of Total Variation Blind Deconvolution. *IEEE Transactions on Pattern Analysis and Machine Intelligence 38*, 6 (2016), 1041–1055. doi:10.1109/TPAMI.2015.2477819. 1

[ŠKB*10] ŠPICLIN Ž., KATRAŠNIK J., BÜRMEN M., PERNUŠ F., LIKAR B.: Geometric calibration of a hyperspectral imaging system. *Applied Optics 49*, 15 (2010), 2813–2818. doi:10.1364/AO.49.002813. 1

[TSAS*19] TONAZZINI A., SALERNO E., ABDEL-SALAM Z. A., HARITH M. A., MARRAS L., BOTTO A., CAMPANELLA B., LEGNAIOLI S., PAGNOTTA S., POGGIALINI F., PALLESCHI V.: Analytical and mathematical methods for revealing hidden details in ancient manuscripts and paintings: A review. *Journal of Advanced Research 17* (2019), 31–42. doi:10.1016/j.jare.2019.01.003. 1